Front. Earth Sci. 2025, 19(3): 452–467
https://doi.org/10.1007/s11707-025-1158-x

RESEARCH ARTICLE

Seismic vulnerability and risk assessment using multimodal data and machine learning: a case study of the central urban area of Jinan City, China

Yaohui LIU[1,2], Xinyu ZHANG[1], Jie ZHOU (✉)[3], Xu HAN[4], Hao ZHENG[5]

1 School of Surveying and Geo-Informatics, Shandong Jianzhu University, Jinan 250101, China
2 Institute of Geology, China Earthquake Administration, Beijing 100029, China
3 School of Geography and Tourism, Qilu Normal University, Jinan 250013, China
4 Research Institute of Highway (Ministry of Transport), Beijing 100088, China
5 Academy of Disaster Reduction and Emergency Management, Faculty of Geographical Science, Beijing Normal University, Beijing 100875, China

Abstract Seismic hazards pose a major threat to life safety, social development, and the economy. Traditional seismic vulnerability and risk assessments, such as field survey methods, may not be suitable for densely built-up urban areas due to the limited availability of comprehensive data and potential subjectivity in judgment. To overcome these limitations, an integrated method for seismic vulnerability and risk assessment based on multimodal remote sensing data, support vector machine (SVM) and GIScience methods was proposed and applied to the central urban area of Jinan City, Shandong Province, China. First, an area with representative buildings was selected for field survey research, and an attribute information base established. Then, the SVM method was used to establish the susceptibility proxies, which were applied to the whole study area after accuracy evaluation. Finally, the spatial distribution of seismic vulnerability and risk under different seismic intensity scenarios (from VI to X) was analyzed in GIScience. The results show that the average building vulnerability index in the central urban area of Jinan City is 0.53, indicating that the overall seismic performance of buildings is at a moderate level. Under the seismic intensity scenario of VIII, the buildings in the Starting area and New urban district of Jinan would mostly suffer 'Moderate' damage, while Old urban areas, with more seismic-resistant buildings, would experience only 'Slight' damage. This study aims to offer an efficient and accurate method for assessing seismic vulnerability in mid to large-sized cities characterized by concentrated population densities and rapid urbanization, as well as provide a valuable reference for efforts in urban renewal, seismic mitigation, and land planning, particularly in cities and regions of developing countries. Additionally, it contributes to the realization of Sustainable Development Goal 11, which seeks to make cities and human settlements inclusive, safe, resilient, and sustainable.

Keywords seismic vulnerability assessment, GIScience, EMS-98, SVM, RISK-UE, multimodal remote sensing data

Received July 4, 2024; accepted March 3, 2025

E-mail: zhoujie_821@163.com

1 Introduction

Seismic hazards, particularly those associated with large, destructive earthquakes, are among the deadliest natural disasters, posing significant threats to international social stability and economic development (Guo, 2010). While seismic hazards pose Geographical location of the study as global challenges, their impact is particularly pronounced in countries like China, Iran, Japan, and Philippines, which are located in active tectonic zones. (Papazafeiropoulos and Plevris, 2023; Perez et al., 2023). China, in particular, has a complex geological structure, active tectonic activity, continuous crustal deformation, and frequent seismic events (Tesfamariam and Liu, 2010; Xu et al., 2013). Studies have shown a positive correlation between building collapse and human casualties in historical seismic events (Li et al., 2014; Liao et al., 2003). Moreover, building vulnerability directly affects their performance during earthquakes (Li et al., 2018). Even under moderate-to-low seismic hazards, highly vulnerable buildings pose a significant seismic risk (Barbat et al., 2006). China has undergone

rapid urbanization in the last decade, becoming a global hotspot for urban growth (Zhang et al., 2018; Adhikari and D'Ayala, 2020). As resources and population continue to concentrate in large cities, potential seismic risks continue to escalate, making risk reduction a critical challenge for sustainable development (Liu et al., 2019). Developing and implementing effective strategies, measures, and interventions to reduce building vulnerability are crucial in mitigating seismic risk (Liu et al., 2020).

The seismic risk assessment of a particular area is related to three fundamental variables: hazard, vulnerability, and exposure (Crichton, 1999; Tyagunov et al., 2004; Cardona et al., 2012). In general, vulnerability is defined as the tendency for a given element to suffer damage or destruction, depending on its inherent physical and functional characteristics (Mouroux and Le Brun, 2006). In seismic risk, the structural features and preservation status of buildings are critical factors influencing vulnerability (D'Ayala, 2013). To enhance the efficiency and accuracy of assessments, researchers have shifted their focus from individual building evaluations to regional-scale building assessments (Tilio et al., 2011), where simplified procedures are often recommended for broader application (Guéguen et al., 2007; Zuccaro and Cacace, 2015). Commonly used vulnerability assessment models include empirical, mechanical, and hybrid methods (Calvi et al., 2006). Empirical methods are determined based on building classification, requiring the use of general data about a group of buildings, such as building type, structural materials, and age of construction (Leggieri et al., 2022). For instance, the EMS-98 macro-seismic scale (Grünthal, 1998) provides guidelines for empirical seismic assessments. Mechanical methods, on the other hand, require detailed information about building geometry, form, and structural characteristics, making their reliability heavily dependent on the accuracy of modeling and input data (Ruggieri et al., 2022). Hybrid methods improve assessment accuracy by calibrating mechanical/analytical evaluations with post-seismic observations of damage (Romano et al., 2017). Despite the advancements in these methods, the reliability of seismic vulnerability assessments depend on the availability and accuracy of the information collected in building inventories (French and Muthukumar, 2006; Yepes-Estrada et al., 2017). Traditional field surveys, though precise and reliable, demand significant manpower and resources, limiting their frequency and efficiency, especially in moderate-to-low seismic hazard areas, where documenting architectural features for individual buildings can be time-consuming and inefficient.

Recently, multimodal data, GIS (Geographic Information System) and remote sensing methods have been integrated and applied to seismic vulnerability assessment at the urban scale, effectively reducing the inherent cost of building surveys (Borfecchia et al., 2010; Boukri et al., 2018; Liu et al., 2023). For instance, Liu et al. (2019) performed the seismic vulnerability assessment of Urumqi City in 2019 by combining data mining methods with GIScience techniques. Salazar and Ferreira (2020) used GIS to collect and manage historical building information in Mexico for seismic vulnerability assessment. Ródenas et al. (2018) used GIS technology to graphically interpret building vulnerability indexes and predict damage, while combining detailed plot characteristics to determine the most vulnerable areas of the city. However, information on building attributes (e.g., type of building structure, age of building, etc.) is not easily determined by visual interpretation of remote sensing imagery alone. Remote sensing methods should be combined with other sources of information to extract relevant parameters (Miura and Midorikawa, 2006; Mueller et al., 2006; Polese et al., 2019). However, these studies mainly focus on the use of GIS and remote sensing technology, and there are few discussions on how to further combine other methods to improve the efficiency and accuracy of assessment.

Machine learning (ML) methods have demonstrated significant potential in the field of seismic vulnerability assessment. Commonly used ML approaches in this domain include supervised learning, unsupervised learning, deep learning, and model integration. Among these, supervised learning techniques such as Decision Trees (DT), SVM, and Artificial Neural Networks (ANN) are widely applied. For example, An et al. (2021) proposed a method to estimate seismic building structure types (SBSTs) in large rural areas by using identification rules and statistical methods based on decision trees, and verified that this method has good accuracy. Riedel et al. (2015) proposed a method to evaluate the seismic vulnerability of buildings on a macro-scale based on data mining technology of SVM and association learning, which can provide a rapid estimate of seismic vulnerability. Yariyan et al. (2020) combined the fuzzy analytic hierarchical process (FAHP) with the ANN model to generate seismic risk assessment (ERA) charts of five vulnerability categories and applied them to Sanandaj City in Iran. The method can accurately identify the highest seismic vulnerability in densely populated areas with dilapidated building infrastructure. Xu et al. (2022) employed ML methods to achieve real-time seismic damage prediction, while Harirchian et al. (2020) optimized a multi-layer perceptron neural network model to evaluate the seismic vulnerability of existing buildings. Other researchers, such as Ruggieri et al. (2021) developed an ML-based framework, VULMA, whose fundamental idea is to process existing photos appropriately to provide data for empirical vulnerability algorithms. Meanwhile, Cardellicchio et al. (2022) used a novel approach to generate the View VULMA data set,

which can enhance the analysis efficiency while maintaining the authenticity of the analysis results. Although the above studies demonstrate the effectiveness of ML and GIS remote sensing technologies, there are still limitations in terms of generalizability and adaptability. Due to the constraints of large individual data sets, the application of existing methods is primarily confined to small-scale scenarios.

To address the above issues, this study aims to develop a cost-effective and highly efficient large-scale building vulnerability assessment model. By integrating urban characteristics with multimodal data (e.g., remote sensing imagery, street view images, land use, and transportation planning data), the model provides a comprehensive assessment of seismic risk for residential buildings on an urban scale. Compared to traditional methods, the proposed approach not only reduces the complexity of collecting building attribute information but also enhances data processing efficiency and assessment accuracy through machine learning techniques such as SVM. This research contributes to strengthening urban resilience against earthquakes, provides valuable insights for government disaster prevention and mitigation efforts, and supports the achievement of the United Nations' Sustainable Development Goals (SDGs). The main contribution of this study is summarized as follows.

1) A building attribute information and seismic vulnerability classification model based on SVM was developed, addressing the bottlenecks of low data processing efficiency and insufficient accuracy in large-scale seismic risk assessments.

2) By integrating the EMS-98 building vulnerability classification standard with the VIM method from the RISK-UE project, seismic risk assessments were conducted under multiple seismic intensity scenarios. The results visually depict the distribution of building damage under varying seismic intensities.

The remainder of the study is organized as follows. Section 2 describes the study area and data sources. Section 3 presents the machine learning approach used for data mining and the methodology used for seismic vulnerability assessment of buildings. Section 4 shows the distribution of building vulnerability and the distribution of seismic damage at different seismic intensities. Discussion and conclusions are presented in Section 5 and Section 6, respectively.

2 Study area and data

2.1 Study area

Jinan, the capital of Shandong Province, China, is situated between 36°01′−37°32′ N and 116°11′−117°44′ E (Fig. 1). As of 2022, Jinan had a population of 9.415 million and covers an administrative area of 10,244 km^2, exhibiting the highest population density of 911 people/km^2 in Shandong Province. The city's terrain is complex, situated on the southern highlands and the northern lowlands, bordered by Mount Tai to the south and the Yellow River to the north. Its geographic location lies in the transitional zone between the central and southern hills of Shandong and the alluvial plains of the north-west. Several faults pass through Jinan and its surroundings, although no major significant active faults exist underground, leading to medium to low seismic risk in the area. In late 2022, Shandong Province issued a "Development Plan for the Jinan New and Old Kinetic Energy Conversion Starting Area (2021−2035)", which redefined the boundaries and scope of Jinan's central urban area. This area is now classified into four regions: the Old city district, the Western new urban district, the Eastern new urban district, and the Starting area for new and old kinetic energy conversion (hereafter referred to as the Starting area). This reclassification aims to expand urban development space, improve resource aggregation efficiency, and facilitate sustainable growth. With a larger transportation network under construction and increasing urban expansion, seismic risk assessment has become a critical component of urban planning.

There are five typical types of building structures in Jinan City, including brick-wood structure, brick-concrete structure, reinforced/confined masonry walls, concrete moment frames, and concrete shear walls. Table 1

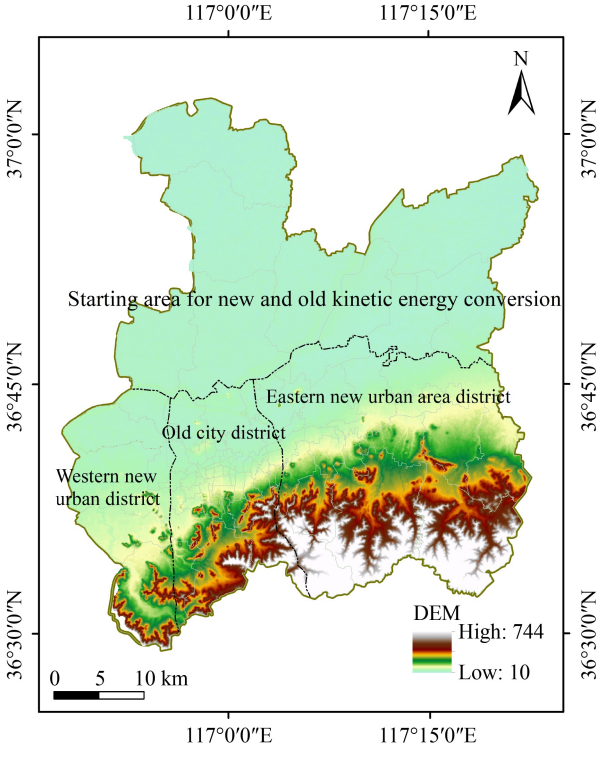

Fig. 1 Geographical location of the study area. The detailed distribution of the center urban area.

presents the types and descriptions of typical buildings in Jinan City.

2.2 Multimodal data

2.2.1 Central urban area database

Considering the factors that may affect the vulnerability of buildings, this study collected data on building attributes, including the type of structure, roof type, number of floors, period of construction, and states of preservation. Multimodal data from diverse sources—such as AOI data of buildings, urban planning information of Jinan City, land use data, road traffic data, and field survey data—were utilized. High-resolution remote sensing images from Google (2×2 m^2 resolution), online maps (e.g., Baidu Maps), street view images, and real estate websites were integrated. This information was compiled into a comprehensive database. AOI data were extracted from Jinan City's urban planning information using Python, incorporating residential community data up to January 2023. To ensure data completeness, missing AOI data for areas such as urban villages and rural settlements were manually supplemented. Buildings with uniform distribution along the same road were classified as the same block and vectorized using Google Earth and street maps. According to urban planning data of Jinan City, the period of construction is divided into four stages: from 2002 to the present, from 1982 to 2002, from 1960 to 1981, and before 1960. Based on the RISK-UE seismic assessment method, the number of floors was classified into three categories: low-rise buildings with two floors or fewer, mid-rise buildings with three to five floors (including five floors), and high-rise buildings with six floors or more. Roof types were divided into flat roofs and sloped roofs. States of preservation are classified into four categories: A (building intact), B (surface peeling), C (wall cracks), and D (non-structural damage), according to specific indicators. Ultimately, the study area was divided into 2518 blocks with uniform building characteristics. Information on the period of construction was obtained from the Real Estate Information Website of Jinan, while data on the number of floors and preservation status were retrieved by combining Baidu panoramic maps and real-time online data. All information was consolidated into a complete database.

The corresponding statistics are as follows: RC1 has 842 buildings (33.4%), RC2 has 673 buildings (26.7%), M4 has 54 buildings (2.2%), M3.3 has 426 buildings (16.9%), and M3.1 has 523 buildings (20.8%). The age of the buildings in Jinan is concentrated from 1982 to 2002. There were 1454 blocks (57.7%) with buildings classified as A based on their state of preservation, while 918 blocks (36.5%) were classified as B. Additionally, 129 blocks (5.1%) were classified as C and 17 blocks (0.7%) were classified as D. After interpreting the remote sensing

Table 1 Typical building types in Jinan City

	**Brick-wood structure** Brick-wood structure uses a combination of brick and timber, with timber serving as supports and beams. This structural system is a variation of unreinforced masonry construction and has better seismic performance compared to traditional unreinforced masonry structures.
	**Brick-concrete structure** Brick concrete structure is a common form of building structure, consisting of concrete walls and bricks. Reinforced concrete has higher strength and stiffness and can bear larger loads and deformations in earthquakes, while brick walls as infill material can increase the stiffness and stability of the structure, thus improving the seismic performance.
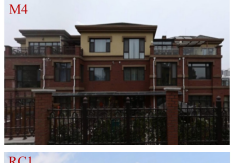	**Reinforced/confined masonry walls** Reinforced masonry walls require higher seismic performance based on building importance, seismic intensity, and other factors. They incorporate more stringent seismic measures and reinforcement designs to ensure superior seismic performance and resistance during earthquakes.
	**Concrete moment frames** Concrete moment frames are a building's common structural system that resists seismic forces during earthquakes. They comprise reinforced concrete beams and columns, connected to form a frame that offers stiffness and strength to the building. These frames can effectively dissipate seismic energy and resist lateral forces, making their seismic performance good.
	**Concrete shear walls** Concrete shear walls are a typical choice for high-rise buildings and other structures, made of reinforced concrete walls. These walls resist lateral forces from seismic activity and wind. Their seismic performance is better than concrete frame structures, as they maintain their structural integrity and resist deformation when subjected to lateral forces caused by an earthquake.

images and street map view images, 1246 buildings were identified as having flat roofs, and 1272 buildings were identified as having sloped roofs. The results are shown in Fig. 2.

2.2.2 Field survey database

Lixia District and Ganggou Street are situated in the southern region of Jinan City with rich landscapes and geographical features. The total area of Lixia District is 100.89 km^2. And as of July 2022, it has 14 streets and 183 communities under its jurisdiction, with a population of about 820000 people. Lixia District is one of the earliest-developed areas in Jinan, characterized by a diverse range of residential building types due to its long history of development. It retains a significant number of historical residential buildings while also featuring modern residential constructions that reflect advancements in building technology and urban planning. As the development center of Jinan, Lixia District provides valuable insights into the evolution of residential architecture. Therefore, it was selected as one of the field survey areas for this study.

Ganggou Street, located in the central area of Licheng District, covers a total area of approximately 107.7 km^2 and is part of Licheng District. It comprises 4 communities and 23 administrative villages, with a population of 117000. Gangou Street is a developing area with many new buildings as well as traditional villages which are still undeveloped. The building types in Lixia District and Ganggou Street are representative of the region as they cover the characteristics of all Jinan area

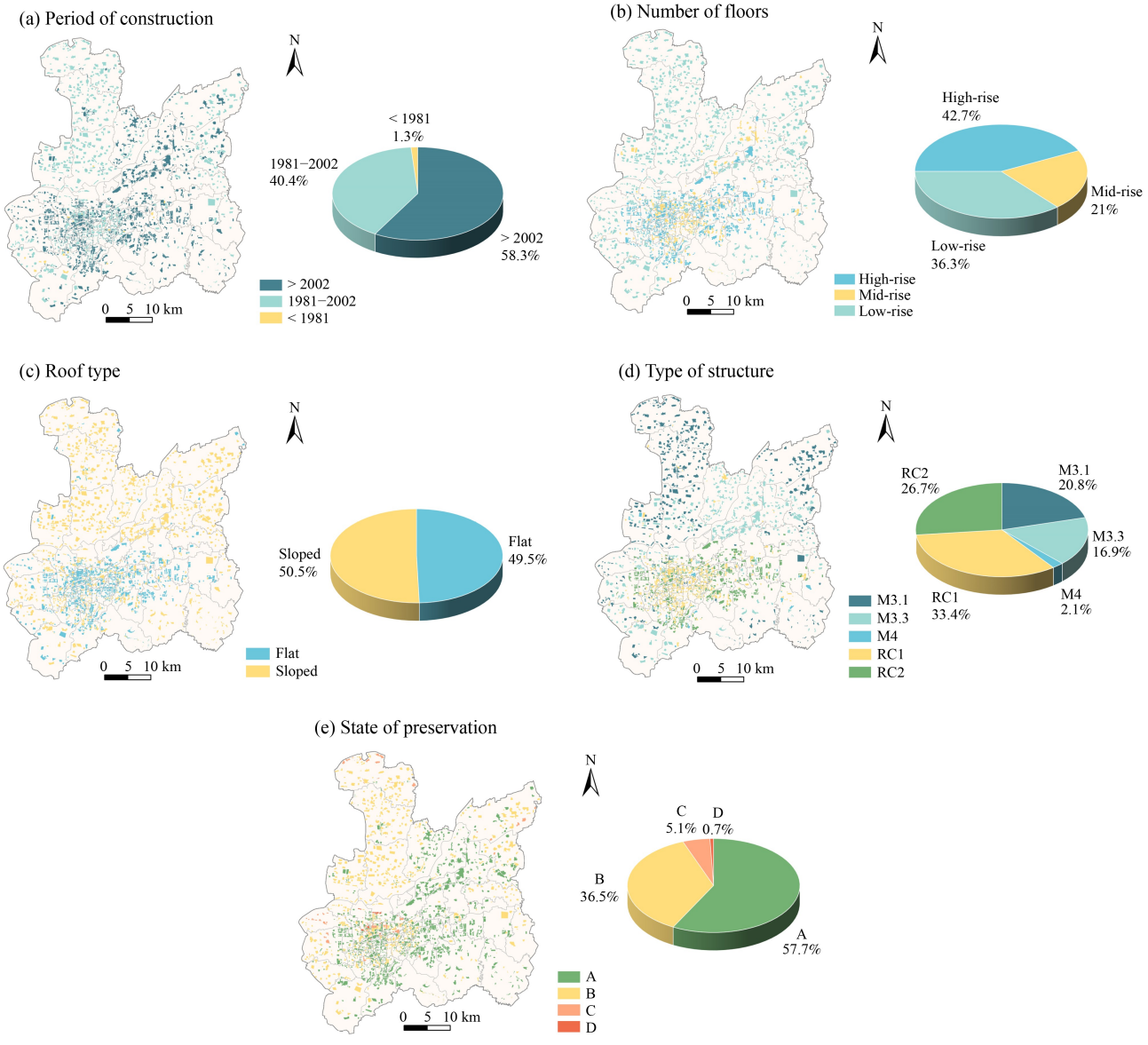

Fig. 2 Spatial distribution and proportion of different attributes in the building database of the Central city of Jinan. (a) Period of construction; (b) number of floors; (c) roof type; (d) type of structure; (d) state of preservation.

buildings. Therefore, they were chosen as the field survey area for this study. The field survey took two weeks, during which detailed building information was collected, and the vulnerability grades of the buildings were recorded.

The EMS-98 scale classifies building vulnerability into six classes, from A (highest) to F (lowest). Using the five attributes of buildings, the vulnerability level of buildings in the field survey area was determined through manual judgment. The results of the vulnerability assessment of buildings in the field survey area are displayed in Fig. 3. The research process of this paper is shown in Fig. 4.

3 Methodology

3.1 EMS-98

EMS-98 is a macro-seismic scale developed by the European Seismological Commission in 1998 to describe the intensity of seismic (Grünthal, 1998). EMS-98 classifies seismic intensity into 12 classes from I to XII based on the degree of damage and impact. Where I is very weakly felt and XII indicates extremely severe seismic damage. In addition to describing seismic intensity, EMS-98 also includes classification criteria for the vulnerability and seismic damage levels.

3.1.1 Vulnerability

Vulnerability refers to the degree of damage and loss sustained by buildings of different structures in the seismic event. It is classified into six levels, from A to F, with A being the most vulnerable and F being the least (Giovinazzi and Lagomarsino, 2004). Vulnerability class F is designed to describe the vulnerability of structures with very strong seismic design levels, i.e., it represents the vulnerability of buildings that have been specially designed for seismic resistance and have high seismic resistance capabilities. However, the number of buildings with special seismic design in the research area is small. The EMS-98 scale first classifies buildings according to their type and then makes finer distinctions based on different design characteristics when considering their seismic performance (Lagomarsino and Giovinazzi, 2006). Generally, the seismic performance of traditional rural masonry structures (structures that have not undergone formal design) is poor, and the most likely range of vulnerability levels is between B and C. The vulnerability level of reinforced concrete structures is most likely to be D. Meanwhile, there are many factors that affect the overall vulnerability of buildings, such as the quality of building materials and construction, preservation status, regularity, location, ductility, and seismic design. Buildings with poor preservation status may not be very sturdy, which could cause a change in vulnerability level by one degree. The assessment of vulnerability in this study depends on factors such as the type of structure, roof type, number of floors, period of construction, and states of preservation. Combined with the EMS-98 scale, the range of vulnerability class values for buildings of each structural type in the study area is shown in Table 2. Vulnerability class is important for assessing seismic risk and disaster prevention. Measures can be taken to improve the seismic resistance of buildings and reduce the damage and casualties caused by seismic based on their vulnerability level.

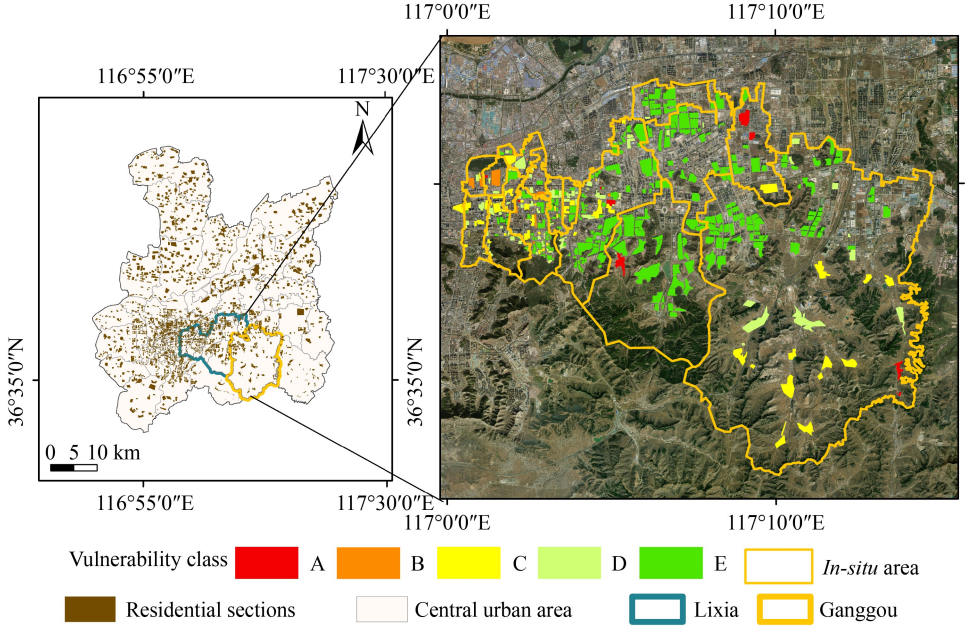

Fig. 3 Field survey area.

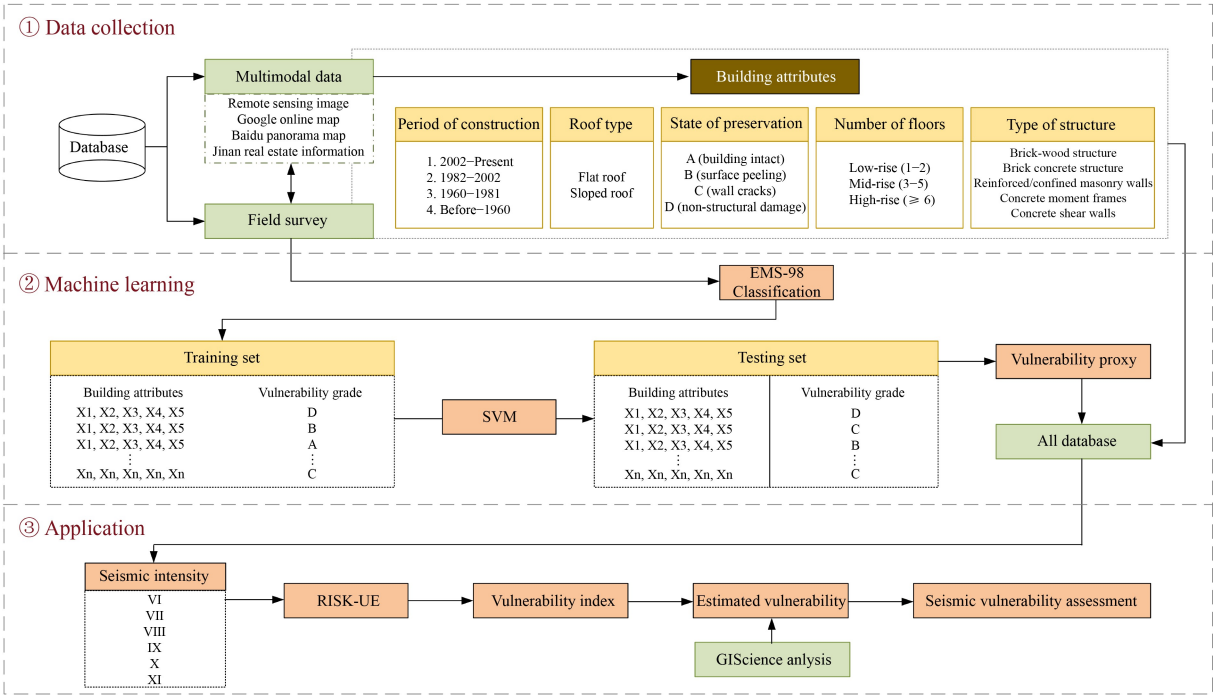

Fig. 4 The schematic workflow of this study.

Table 2 The range of vulnerability values corresponding to different structural types of buildings

Type of Structure		Vulnerability class A	B	C	D	E	F
Masonry	Brick-wood structure	◀- - - ● ——▶					
	Brick concrete structure		◀- - - ● ——▶				
	Reinforced masonry walls		◀- - - ● ——▶				
				◀- - - ● ——▶			
Reinforced concrete (RC)	Concrete shear walls			◀- - - ● ——▶			
					◀- - - ● ——▶		

● most likely vulnerability class; ——▶ probable range; - - - ▶ range of less probable, exceptional cases.

3.1.2 Seismic damage level

The classification of seismic damage levels describes the possible negative effects of seismic events on humans and society. According to the EMS-98 scale, there are five levels of seismic damage: DG1 (slight damage), DG2 (moderate damage), DG3 (substantial to heavy damage), DG4 (severe damage), and DG5 (destruction).

3.2 SVM

ML can enhance the performance of algorithms by utilizing empirical learning, thereby bringing the program performance closer to the desired criteria (Jordan and Mitchell, 2015). Typically, ML involves analyzing large observational data sets to identify correlations among different data for summarization, and can achieve high accuracy within a short period of training. In recent years, ML methods have experienced significant advances, with techniques such as deep learning, big data, computer vision, and natural language processing being widely employed across diverse domains. SVM were proposed by Cortes (Cortes and Vapnik, 1995) mainly used for solving classification and regression problems. In this study, the building attribute data corresponding to vulnerability are divided into training and test sets, and the best proxy between the data is found by SVM, which is then applied to the whole study area. The study is divided into four main phases: data processing, training, validation, and application. The association proxy between building attribute information and vulnerability is used to infer the vulnerability of large-scale buildings,

which can greatly reduce the cost of vulnerability analysis of urban-scale buildings.

The primary objective of SVM is to find the optimal hyperplane, i.e., the maximum interval of the decision boundary (Yang et al., 2015). Consider a set of training samples: $(y_1, x_1), ..., (y_l, x_l)$, where $y_i \in \{-1, 1\}$. An inequality is satisfied by each element if there exists a vector w and a scalar b:

$$w \times x_i + b \geqslant 1 \text{ if } y_i = 1, \tag{1}$$

$$w \times x_i + b \leqslant -1 \text{ if } y_i = -1. \tag{2}$$

The distance of a point from the hyperplane can be described functionally as

$$y_i(w \times x_i + b) \geqslant 1 i = 1, ..., l. \tag{3}$$

The optimal hyperplane is the classification surface that achieves maximum classification interval and accurately classifies the two categories. The optimal parameters, denoted by w_0 and b_0, define the optimal hyperplane as follows:

$$w_0 \times x + b_0 = 0. \tag{4}$$

The classification interval is

$$\rho(w, b) = \min_{\{x:y=1\}} \frac{x \times w}{|w|} - \max_{\{x:y=1\}} \frac{x \times w}{|w|}. \tag{5}$$

The maximum geometric distance between the projections of two training vectors of different classes can be expressed as

$$\rho(w_0, b_0) = \frac{2}{|w_0|} = \frac{2}{\sqrt{w_0 \times w_0}}. \tag{6}$$

To simplify, the maximum geometric distance can also be expressed as

$$\max \frac{1}{2} w^2. \tag{7}$$

The SVC algorithm in SVM consists of two kernel functions, the polynomial kernel function (PLOY) and the Radial basis function (RBF). RBF also known as the radial basis function, which essentially maps each sample point to an infinite-dimensional feature space, making linearly indistinguishable data linearly divisible, and thus finding the optimal hyperplane or decision boundary (Schwenker et al., 2001). The advantage of using the kernel function is that it can avoid repeatedly calculating the specific mapping of sample points in the high-dimensional space in the SVM, improving the efficiency of SVM computation and reducing the storage space occupation (Pourghasemi et al., 2013):

$$K(x, y) = e^{-\gamma \|x-y\|^2}, \gamma > 0, \tag{8}$$

where $K(x, y)$ is the kernel function and γ is the hyperparameter in RBF, the larger its value, the higher the model complexity. Improper values of x can lead to overfitting or underfitting of the model. The value of γ in the experiment is taken as 0.2 after training. $\|x-y\|$ is the mode of the vector. The formula for the definition of RBF is the formula for the dot product. The class label of the training set in the study is vulnerability classification, and the five features correspond to the type of structure, period of construction, roof type, number of floors, and period of construction, respectively. In the supervised classification framework, SVM is applied to establish the optimal hyperplane for fragility classification. The classification results are evaluated based on the confusion matrix.

3.3 RISK-UE

RISK-UE is an EU-funded study project aimed at improving urban seismic risk management and disaster reduction capabilities to reduce the risk of urban seismic disasters (Milutinovic and Trendafiloski, 2003). RISK-UE includes two methods: the statistical method for vulnerability and seismic risk assessment of buildings (LM1) and the physical method for seismic risk assessment (LM2) (Bektaş and Kegyes-Brassai, 2022). The LM1 method mainly evaluates the seismic performance of buildings based on structural parameters such as building type, material, and height, which is highly compatible with the EMS-98 scale. It is divided into six levels of seismic damage: none, slight, moderate, substantial to heavy, very heavy, and destruction. It is generally used for macro-scale seismic risk assessment. The LM2 method focuses more on the characteristics of the seismic event itself, such as the distance from the epicenter and the magnitude, while also considering the structural parameters of the building. This method is mainly used for real-time seismic risk assessment and emergency response planning. As Jinan City is a moderate-to-low risk area, the Vulnerability Index Method (VIM) of the LM1 method was selected for calculation in this study. The calculation process can be divided into the following three steps.

1) Estimate the vulnerability index ($\overline{V_I}$)

The Building Typology Matrix (BTM) is a method of classifying buildings according to their physical characteristics and structural properties and is an important component of VIM (Lantada et al., 2010). Its purpose is to simplify and standardize the assessment process, as well as improve the accuracy of estimating the vulnerability index and average seismic rating of buildings. The vulnerability index ranges from 0 and 1, with lower values indicating a reduced level of vulnerability. The vulnerability index is classified based on the building structure type and is associated with the median ($V^*_{I,BTM}$), minimum reasonable limit ($V^-_{I,BTM}$), and

maximum reasonable limit ($V^{+}_{\mathrm{I,BTM}}$) of possible vulnerability index values. Table 3 displays the matching values for the building structure types in the study area and their corresponding classifications in the RISK-UE method.

The value of the vulnerability index is also related to factors such as the geographical location of the building, its height, and the irregularity of complex buildings. Eq. (9) is a modified calculation for the fragility index. Where V^{*}_{I} represents the most likely value for different structural types of buildings. ΔV_{R} is the regional vulnerability factor, which includes special qualities at the regional scale such as geological conditions, meteorological conditions, and socio-economic conditions. ΔV_{M} is the seismic behavior modification factor, which mainly considers the actual energy dissipation capacity, deformation capacity, and seismic performance of the building. The regional vulnerability factor and the seismic behavior modification factor are not considered in this study:

$$\overline{V_{\mathrm{I}}} = V^{*}_{\mathrm{I}} + \Delta V_{\mathrm{R}} + \Delta V_{\mathrm{M}}. \tag{9}$$

2) Estimate the mean seismic damage grade μ_D

According to the vulnerability index $\overline{V_{\mathrm{I}}}$ and the corresponding seismic intensity I, the mean seismic damage grade μ_{D} is estimated using the following formula:

$$\mu_{\mathrm{D}} = 2.51 + \tanh\frac{I + 6.25\overline{V_{\mathrm{I}}} - 13.1}{\varnothing}. \tag{10}$$

The seismic intensity is represented by I, and the ductility index ϕ is considered, which is determined based on the building type and assigned a value of 2.3 for buildings. The mean seismic damage index $\overline{\mu_{\mathrm{D}}}$ is calculated using the following formula:

$$\overline{\mu_{\mathrm{D}}} = \sum_{k=0}^{5} p_k k. \tag{11}$$

The seismic damage grade is denoted by k and takes values ranging from 0 to 5. The probability associated with each seismic damage grade is represented by p_k.

3) Estimate the damage distribution

Assuming a given seismic intensity, the prediction of the damage grade follows a binomial distribution, and the probability calculation for each grade is expressed as follows:

$$P(D_k) = \frac{5!}{k!(5-k)!}\left(\frac{\mu_{\mathrm{D}}}{5}\right)^{k}\left(1 - \frac{\mu_{\mathrm{D}}}{5}\right)^{5-k}. \tag{12}$$

Table 3 Vulnerability index values for various buildings based on RISK-UE

Typology	V^{*}_{I} representative values				
	$V^{\min}_{\mathrm{I,BTM}}$	$V^{-}_{\mathrm{I,BTM}}$	$V^{*}_{\mathrm{I,BTM}}$	$V^{+}_{\mathrm{I,BTM}}$	$V^{\max}_{\mathrm{I,BTM}}$
RC1	−0.020	0.047	0.442	0.800	1.020
RC2	−0.020	0.047	0.386	0.670	0.860
M3.1	0.460	0.650	0.74	0.830	1.020
M3.3	0.460	0.527	0.704	0.830	1.020
M4	0.140	0.33	0.451	0.633	0.700

4 Seismic vulnerability assessment results

4.1 SVM application

4.1.1 SVM training

After the buildings in the field survey database were classified according to vulnerability, the data was then divided into a training set and a test set for the SVM method. To determine the optimal amount of data to train, experiments were conducted using training sets of 10%, 20%, 30%, 40%, 50%, 60%, and 70%. Before each experiment, data were randomly selected to form the training set to ensure the experimental reliability. Each set of experiments was repeated independently 1000 times to generate 1000 mutually independent training and test sets. The accuracy of each set of experiments was recorded, and the average accuracy and dispersion of experiments with different amounts of data training were calculated. The results, shown in Fig. 5, indicate that as the amount of training data increased, the overall accuracy also improved. However, the dispersion exhibited a trend of initially decreasing and then increasing, likely due to changes in sample diversity and the potential for overfitting in larger data sets. Based on the highest overall accuracy and the lowest dispersion, the optimal amount of data was determined to be 50% of the training set. In all experiments with different attribute combinations, 50% of the data volume was selected as the training set.

The accuracy of the training model can be affected by the combination of building attributes, which was

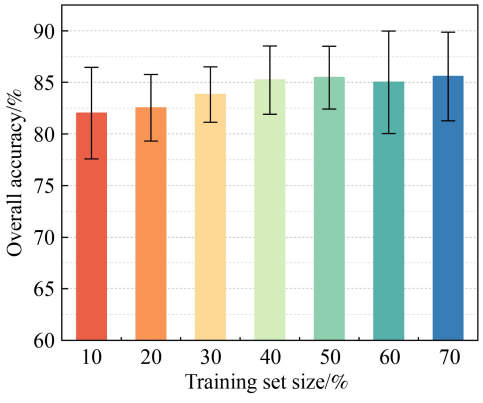

Fig. 5 The accuracy and dispersion among the different sets of training sizes.

investigated in this study through experiments using different attribute combinations with a training sample size of 50%. For experiments considering only two attributes, the average accuracy of the combination of Fig. 6(a) (period of construction and number of floors) was 81.85%; for Fig. 6(b) (roof type and number of floors), it was 68.69%; and for Fig. 6(c) (state of preservation and number of floors), it was 76.62%. These results indicate that the period of construction and number of floors have a more significant impact on seismic vulnerability, while roof type has the least.

When considering the three attributes, the average accuracy for the combination of Fig. 6(d) (roof type, period of construction, number of floors) was 81.36%; for Fig. 6(e) (period of construction, number of floors, type of structure), it was 84.71%, and for Fig. 6(f) (period of construction, state of preservation, type of structure) reaches 85%. A comparison of these three combinations shows that structural type is an important factor in the assessment of seismic vulnerability, as seen in previous (Lang, 2002). This was also confirmed in the study.

When considering the four attributes, the classification accuracy for the combination of Fig. 6(g) (period of construction, number of floors, type of structure, roof type) was 85.41%, compared to 85.38% for the combination of Fig. 6(h) (period of construction, number of floors, type of structure, state of preservation). Compared to the training results for the three attribute combinations, the accuracy for the four attribute combinations improved. When all five attributes were trained, the average accuracy obtained reached 85.46%. These results suggest that increasing the number of building attributes used in the training model generally improves accuracy, with diminishing returns beyond four attributes. Period of construction, number of floors, and type of structure were identified as the most critical factors in assessing seismic vulnerability, while roof type had the least impact.

4.1.2 SVM validation

Confusion matrix is a widely used tool in classification

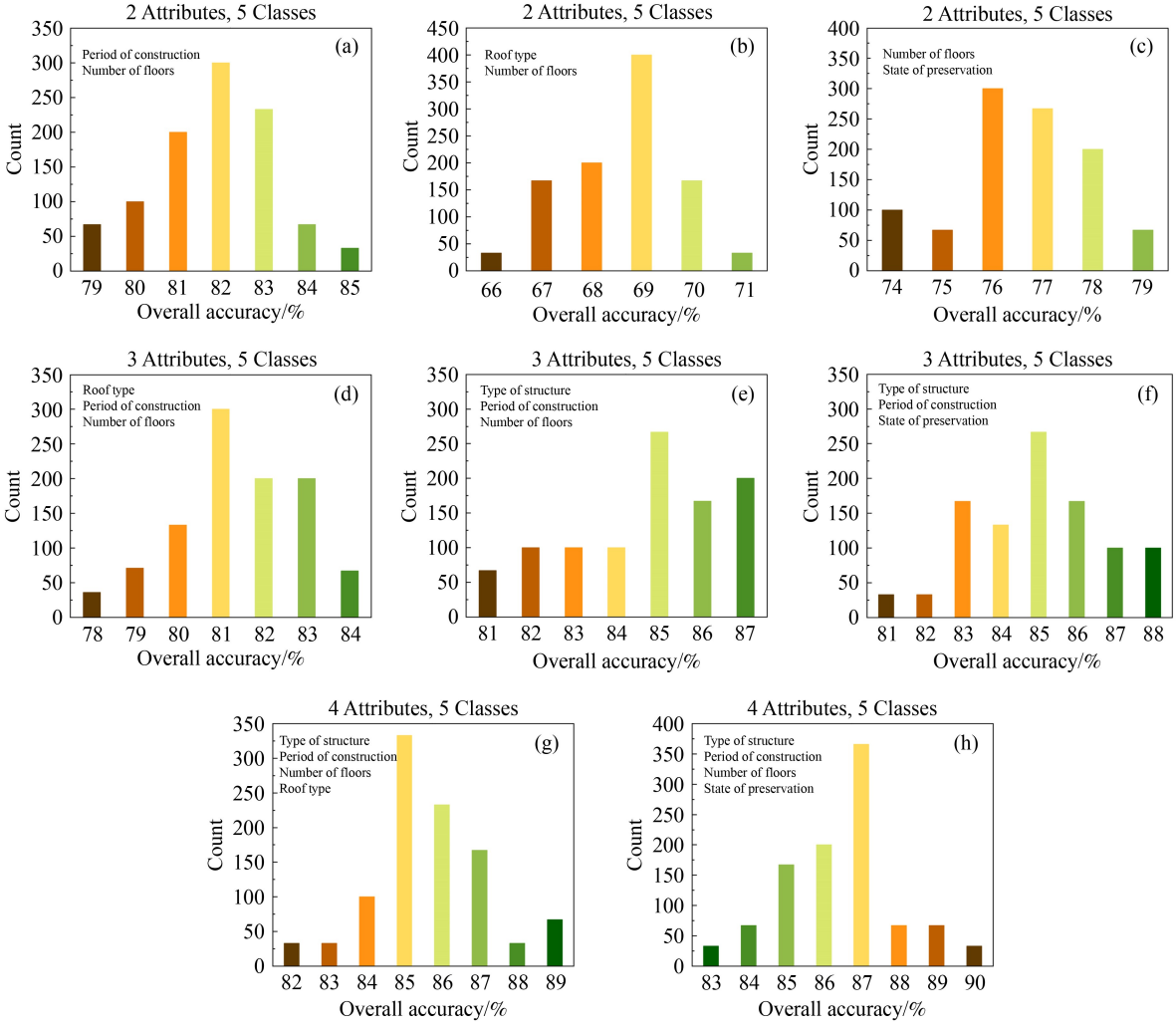

Fig. 6 Overall accuracy of different combinations of building attribute.

task to evaluate the quality of classification algorithm (Susmaga, 2004). It is generated by comparing the predicted results of the model with the actual results. In the matrix, rows represent the actual categories, while columns represent the predicted categories. In this study, the confusion matrix was derived from the classification results of the training model using five attributes in the field survey data set, as shown in Fig. 7. The overall accuracy of the classifier was found to be 85.98%. The value on the diagonal of the confusion matrix represents the accuracy of each vulnerability class classification. It was observed that the classification accuracy of Class A and Class E buildings was higher as almost all of them were identified correctly. However, the classification accuracy of Class B and Class C was comparatively lower, which can be attributed to the small amount of Class B and Class C data in the data set. In general, the overall performance of the training model met the requirements of the experiment.

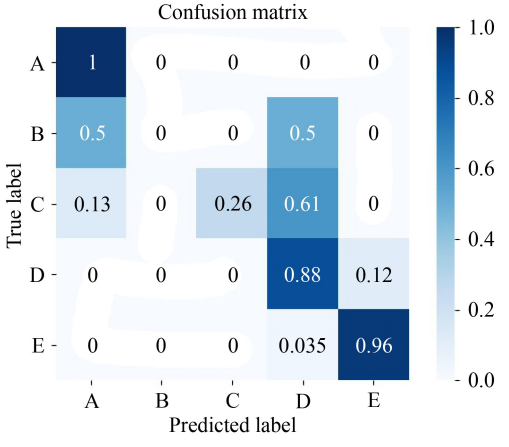

Fig. 7 Confusion matrix obtained by SVM training using five attributes.

4.1.3 Seismic vulnerability distribution

After the SVM training stage, a set of seismic vulnerability proxy sets corresponding to five building attributes was established and applied to the entire central urban area. GIS has advantages in seismic risk assessment, such as data integration, spatial analysis, and visualization. It can display the distribution of buildings intuitively, which is helpful for urban management and planning. The spatial distribution of vulnerability in the central urban area is shown in the GIS platform, as illustrated in Fig. 8. The results indicate that the seismic performance of buildings located in the northern edge of the central city is the worst, with the majority being classified as either A or B. Buildings with a vulnerability of C are widely distributed in the southern fringe. In contrast, buildings in the central region, which has undergone rapid economic development, exhibit the best seismic performance, with the majority being classified as D and E.

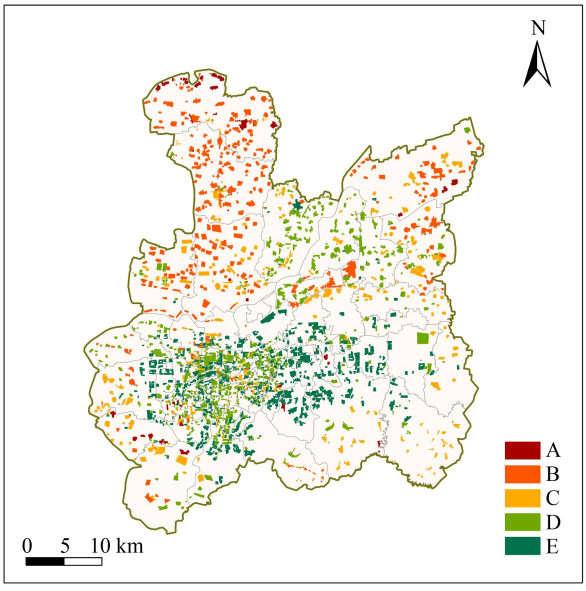

Fig. 8 Spatial distributions of EMS-98 vulnerability obtained with the SVM.

4.2 Seismic risk assessment in Jinan City

4.2.1 Vulnerability index

According to Eq. (9), the vulnerability index of the study area is concentrated between 0.39 and 0.74, with an average value of 0.53. This means that the buildings in the area generally have medium to high seismic resistance, but a certain proportion of buildings are still vulnerable to seismic damage. When combined with the spatial distribution diagram of the vulnerability index (Fig. 9), it can be observed that buildings with high vulnerability indices are mainly concentrated in the Starting area and on the edges of the Eastern and Western new urban areas. The majority of these areas are rural, and the housing primarily consists of M3.1 and M3.3 structures lacking seismic fortification measures. On the contrary, in areas that experienced early economic development, such as the Old city district and its surrounding areas, most buildings were converted into frame structures, leading to lower vulnerability to seismic damage.

4.2.2 Seismic risk analysis

Different seismic intensities would have varying effects on the average seismic damage degree. The intensity of a seismic event is typically directly proportional to the energy and frequency of the seismic waves, resulting in a stronger dynamic response of the building structure, and consequently, increasing the likelihood of severe damage.

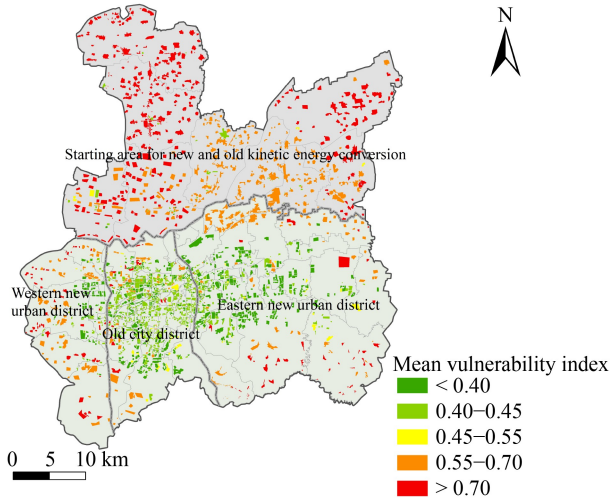

Fig. 9 Spatial distribution of the seismic vulnerability index.

Therefore, evaluating the average seismic damage under different seismic intensities is crucial. According to the RISK-UE method, the seismic damage degree of buildings was divided into six grades, ranging from "None" to "Destruction". The corresponding relationship between the average seismic damage index and seismic damage degree classification is shown in Table 4.

After obtaining the susceptibility index, the average degree of seismic damage under seismic intensity (VI to XI) was calculated using Eq. (10) in ArcGIS platform. The spatial distribution of calculation results is shown in Fig. 10. Figure 10(a) illustrates the spatial distribution of seismic damage for seismic intensity VI, with an average seismic damage index ranging from 0.08 to 0.52. The degree of seismic damage is generally very low, with "" None" and "Slight" being the main seismic damage levels. Only a few buildings, mostly located to the east and west of the Starting area, were slightly damaged. For seismic intensity VII, as shown in Fig. 10(b), the damage index is concentrated between 0.2 and 1.09. The number of "Slight" damaged buildings increased compared to the previous intensity level, with widespread minor damage to buildings, and only a small number of undamaged buildings mainly concentrated in central areas. When the seismic intensity reached VIII, as depicted in Fig. 10(c), "Moderate" damaged buildings began to appear. Most of the buildings in the Starting area, Western and Eastern new urban district suffered "Moderate" damage, while "Slight" damage was predominant in the central region. Only a few buildings with strong seismic resistance were not damaged. When the seismic intensity reaches IX, as depicted in Fig. 10(d), the mean seismic damage index is 1.79, with "Slight" and "Substantial to Heavy" being the main degrees of seismic damage and an overall damage degree of "Moderate". It can be observed that buildings in the northern region suffered "Substantial to Heavy" seismic damage, while the buildings in the southern region were mainly "Slight" damaged. When the seismic intensity reaches X, as depicted in Fig. 10(e), the average value of the seismic damage index is 2.7, with an overall degree of seismic damage in the study area being "Substantial to Heavy". At the same time, the buildings in the northern region and the buildings in the southern marginal region suffered serious structural damage and could not continue to be occupied. Figure 10(f) shows that when the seismic intensity reaches XI, the average seismic damage index exceeds 3.5, with almost all buildings having structural damage, and the whole city being destroyed. The proportions of damage grades under different seismic intensities are shown in Fig. 11. The results indicate that when the seismic intensity ranges from VI to IX, the damage level of buildings is mainly classified as "None" and "Slight". Among them, the proportion of buildings that experienced "Slight" damage at seismic intensity IX is the highest, accounting for about 31%. In areas with seismic intensity X, a considerable portion of buildings experienced "Very Heavy" damage, accounting for about 50%. When the seismic intensity reaches XI, all buildings were damaged at "Substantial to heavy" and "Very Heavy" levels. The overall trend indicates that the level of damage to buildings increases gradually with the increase of seismic intensity.

In summary, the use of GIS in seismic risk assessment provides valuable advantages such as data integration, spatial analysis, and visualization, which can directly display the spatial distribution of seismic damage and contribute to urban management and planning. The results of the study showed that different seismic intensities have a significant impact on the degree of seismic damage, with more severe intensities resulting in more complex and stronger dynamic responses of

Table 4 Mean damage index values and corresponding damage states

Mean damage index interval	Most probable damage state	Description
0.0−0.5	None	No damage
0.5−1.5	Slight	Negligible to slight damage
1.5−2.5	Moderate	Slight structural, moderate non-structural
2.5−3.5	Substantial to Heavy	Moderate structural, heavy non-structural
3.5−4.5	Very Heavy	Heavy structural, very heavy non-structural
4.5−5.0	Destruction	Very heavy structural, total, or nearly total collapse

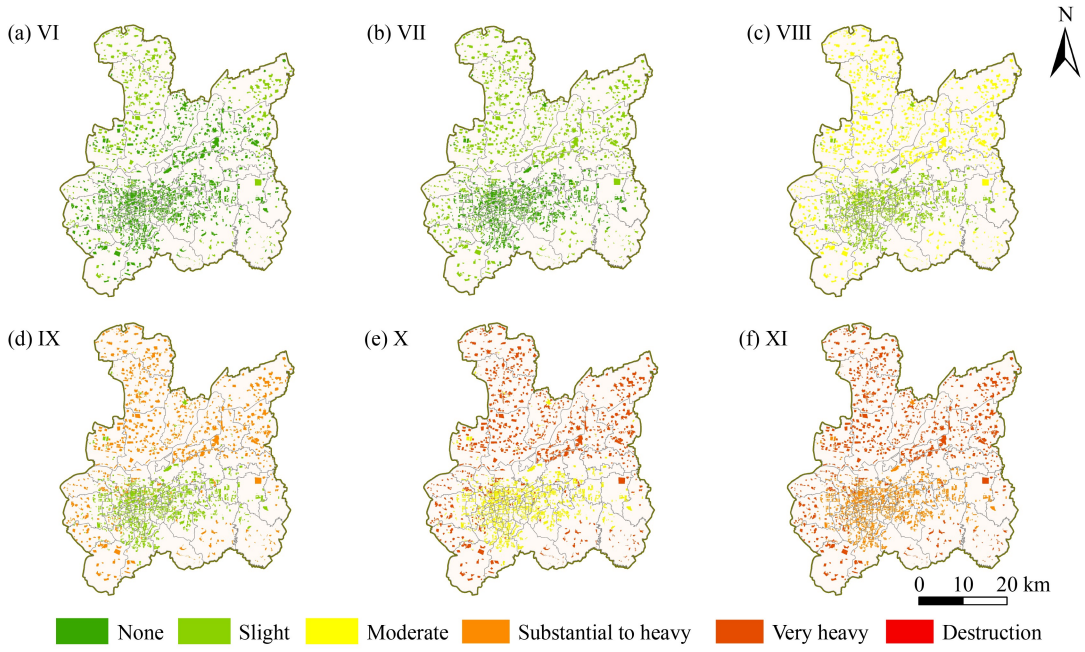

Fig. 10 The spatial distribution of seismic damage grade under different seismic intensities.

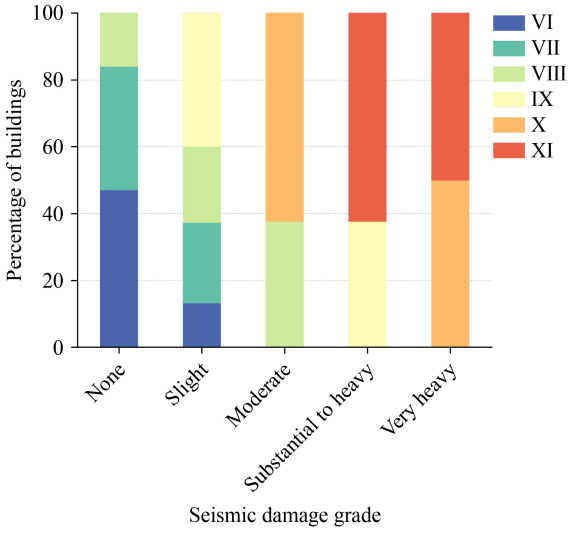

Fig. 11 The proportions of damage grades under different seismic intensities.

building structures and causing more serious damage. The spatial distribution of seismic damage was analyzed for different intensities, ranging from "None" and "Slight" damage at intensity VI to widespread "Substantial to Heavy" damage at intensity IX, and ultimately leading to the destruction of the entire city at intensity XI.

5 Discussion

This study proposes a seismic vulnerability assessment method for buildings in rapidly urbanizing areas, such as Jinan, spanning from individual buildings to blocks and ultimately to the urban scale. Residential units were divided into residential blocks, considering the relationships among buildings, roads, and planning, with the assumption that internal buildings share the same attributes. The vulnerability levels were evaluated based on the EMS-98 scale, and a reliable database was established.

The study integrated multimodal data and field survey-derived building attributes to employ the SVM method for training and testing. The optimal proxy combination between building attributes and vulnerability levels was identified and subsequently applied to the urban scale. The results show that the SVM method demonstrates stability and high accuracy in vulnerability assessment, making it advantageous for conducting vulnerability assessments in data-limited situations.

The findings of this study demonstrate the distribution of buildings with poor seismic performance in Jinan's central urban area and the spatial pattern of damage under seismic intensities ranging from VI to XI. Significant differences in building damage levels across regions can be attributed to variations in building structure types, construction periods, and economic development levels. Buildings in rural areas, often constructed with outdated brick-wood and brick-concrete structures lacking seismic fortification, exhibit poor seismic performance and are highly susceptible to damage during earthquakes. In contrast, buildings in new urban areas predominantly adopt frame-shear wall structures, characterized by higher construction quality and modern seismic design, resulting in better overall seismic performance. Furthermore, economically developed areas such as the old urban district and its surrounding regions have undergone urban

renewal and reconstruction, leading to the widespread adoption of frame structures and modern seismic designs. Consequently, these areas exhibit lower vulnerability indices.

Seismic risk assessment involves several uncertainties, such as the probability of earthquake occurrence, magnitude, focal depth, and the complexity and diversity of building structures, all of which may affect the assessment results. Additionally, this study assumes uniform building attributes within a block, which is a simplified assumption that may overlook subtle differences between buildings within the same region, potentially impacting assessment accuracy. Future research should incorporate uncertainty analyses, such as sensitivity analysis or Monte Carlo simulations, to quantify the robustness of the assessment results. Moreover, deep learning technologies could be integrated to further improve the efficiency of data acquisition and processing, for instance, by using remote sensing images to automatically extract building information. This would reduce manual intervention costs and enhance the accuracy and applicability of the assessment results.

Furthermore, future research should perform broader data validation to improve the reliability and generalizability of the assessment results. Specifically, more detailed seismic damage data could be collected from other large-scale cities that have experienced major earthquakes. By comparing and validating the proposed method under varying geographic and building conditions, the applicability and robustness of the method can be evaluated. This will help optimize model parameters, enhance the generalizability of the assessment method, and provide scientific support for seismic vulnerability assessment at regional and even global scales.

In conclusion, the method proposed in this study offers a low-cost, high-efficiency solution for assessing building vulnerability in regions with low to moderate seismic risk, demonstrating strong practical application value. Future work can focus on optimizing the method, reducing uncertainty impacts, and promoting its application in cities with diverse seismic risk contexts.

6 Policy and practical recommendations

Based on the findings of this study, the following policy and practical recommendations are proposed. 1) Strengthening Seismic Retrofitting for High-Vulnerability Buildings: priority should be given to seismic evaluation and retrofitting projects for buildings in the northern Starting Area and rural areas in the north-west and south-west. 2) Optimizing Urban Planning and Renewal: urban renewal projects should implement high seismic standards, replacing or retrofitting old buildings. 3) Enhancing Disaster Warning and Emergency Management: evacuation plans for key areas should be developed using GIS-based analysis to improve emergency response efficiency.

For densely populated cities and regions with rapid urbanization, it is essential to scientifically improve urban seismic performance through efficient and cost-effective methods.

7 Conclusions

In this study, we conducted a seismic vulnerability and risk assessment in the central urban area of Jinan City through a comprehensive and integrated method employing multimodal data and ML. First, multimodal data including remote sensing images, land and transportation planning data, and street view images, were used to collect building attribute information instead of traditional field survey methods. An *in situ* area was selected to determine the vulnerability of buildings based on the EMS-98 scale. Next, the best proxy between building attributes and vulnerability was established using the SVM method and applied to the entire study area to obtain the vulnerability of the entire area. Lastly, the degree of destruction of buildings in Jinan City at various seismic intensities of VI, VII, VIII, IX, X, and XI was calculated and displayed in the GIS environment. The main conclusions of this study are as follows.

1) After applying the best proxy between building attributes and vulnerability to the entire study area, the spatial distribution of vulnerability shows that there are few buildings with vulnerability level A (most vulnerable). Most of these buildings are distributed in the north-west and south-west rural areas of Jinan.

2) The average VIM index of the central urban area of Jinan is 0.53, indicating that the seismic performance of buildings is generally satisfactory. However, the seismic performance of some buildings in certain areas, such as the Starting area in the north and the edge areas of the East and West new urban areas, is deficient.

3) When the seismic intensity is below level VIII, the city suffers only “Moderate” damage. When the seismic intensity reaches level IX or above, the damage to the urban area is severe. At this point, the structural damage to buildings will be more severe, and many buildings may be unusable. When the seismic intensity reaches level IX or above, residents in the city need to evacuate immediately to avoid possible catastrophic consequences, especially in the Starting area and the old densely populated urban areas.

This study provides a reference for seismic vulnerability assessments in developing countries, helping to mitigate direct economic losses from earthquakes. It also supports SDG 11, emphasizing its practical significance.

Authorship contribution Yaohui Liu conceived the idea and designed the experiments. Xinyu Zhang conducted the data analysis and contributed to the writing of the manuscript. Jie Zhou and Xu Han collected the research data and assisted in data interpretation. Hao Zheng provided critical revisions and guidance throughout the manuscript preparation.

Acknowledgement We would like to thank the editors and the anonymous reviewers for their insightful comments and suggestions. This study was supported in part by the National Natural Science Foundation of China (Grant No. 42201077); the Natural Science Foundation of Shandong Province (No. ZR2021QD074); the China Postdoctoral Science Foundation (No. 2023M732105); the Lhasa National Geophysical Observation and Research Station (No. NORSLS22-05); the Youth Innovation Team Project of Higher School in Shandong Province, China (No. 2024KJH087).

Competing interests The authors declare that they have no competing interests.

Data availability Data will be made available on request.

References

Adhikari R K, D'Ayala D (2020). 2015 Nepal earthquake: seismic performance and post-earthquake reconstruction of stone in mud mortar masonry buildings. Bull Earthquake Eng, 18(8): 3863–3896

An J, Nie G, Hu B (2021). Area-wide estimation of seismic building structural types in rural areas by using decision tree and local knowledge in combination. Int J Disaster Risk Reduct, 60: 102320

Barbat A H, Pujades L G, Lantada N (2006). Performance of buildings under earthquakes in Barcelona, Spain. Comput Aided Civ Infrastruct Eng, 21(8): 573–593

Bektaş N, Kegyes-Brassai O (2022). Conventional RVS methods for seismic risk assessment for estimating the current situation of existing buildings: a state-of-the-art review. Sustainability (Basel), 14(5): 2583

Borfecchia F, Pollino M, De Cecco L, Lugari A, Martini S, La Porta L, Ristoratore E, Pascale C (2010). Active and passive remote sensing for supporting the evaluation of the urban seismic vulnerability. Italian Journal of Remote Sensing, 42(3): 129–141

Boukri M, Farsi M N, Mebarki A, Belazougui M, Ait-Belkacem M, Yousfi N, Guessoum N, Benamar D A, Naili M, Mezouar N, Amellal O (2018). Seismic vulnerability assessment at urban scale: case of Algerian buildings. Int J Disaster Risk Reduct, 31: 555–575

Calvi G M, Pinho R, Magenes G, Bommer J, Restrepo-Veiez L F, Crowley H (2006). Development of seismic vulnerability assessment methodologies over the past 30 years. ISET J Earthquake Technol, 43(3): 75–104

Cardellicchio A, Ruggieri S, Leggieri V, Uva G (2022). View VULMA: data set for training a machine-learning tool for a fast vulnerability analysis of existing buildings. Data (Basel), 7(1): 4

Cardona O D, Van Aalst M K, Birkmann J, Fordham M, Mc Gregor G, Rosa P, Pulwarty R S, Schipper E L F., Sinh B T, Décamps H, Keim M, Davis I, Kristie L. Ebi, Lavell A, Mechler R, Murray V, Pelling M, Pohl J, Smith A O, Thomalla F (2012). Determinants of Risk: Exposure and Vulnerability. Cambridge: Cambridge University Press

Cortes C, Vapnik V (1995). Support-vector networks. Mach Learn, 20(3): 273–297

Crichton D (1999). The risk triangle. Natural Disaster Management, 102(3): 102–103

D'Ayala D (2013). Assessing the seismic vulnerability of masonry buildings. In: Goda K, Tesfamariam S, eds. Handbook of Seismic Risk Analysis and Management of Civil Infrastructure System. New York: Woodhead Publishing

French S P, Muthukumar S (2006). Advanced technologies for earthquake risk inventories. J Earthquake Eng, 10(2): 207–236

Giovinazzi S, Lagomarsino S (2004). A macroseismic method for the vulnerability assessment of buildings. In: 13th World Conference on Earthquake Engineering. Canada Vancouver

Grünthal G (1998). European macroseismic scale 1998: EMS-98. European Seismological Commission (ESC)

Guéguen P, Michel C, LeCorre L (2007). A simplified approach for vulnerability assessment in moderate-to-low seismic hazard regions: application to Grenoble (France). Bull Earthquake Eng, 5(3): 467–490

Guo H (2010). Understanding global natural disasters and the role of earth observation. Int J Digit Earth, 3(3): 221–230

Harirchian E, Lahmer T, Rasulzade S (2020). Earthquake hazard safety assessment of existing buildings using optimized multi-layer perceptron neural network. Energies, 13(8): 2060

Jordan M I, Mitchell T M (2015). Machine learning: trends, perspectives, and prospects. Science, 349(6245): 255–260

Lagomarsino S, Giovinazzi S (2006). Macroseismic and mechanical models for the vulnerability and damage assessment of current buildings. Bull Earthquake Eng, 4(4): 415–443

Lang K (2002). Seismic Vulnerability of Existing Buildings. vdf Hochschulverlag

Lantada N, Irizarry J, Barbat A H, Goula X, Roca A, Susagna T, Pujades L G (2010). Seismic hazard and risk scenarios for Barcelona, Spain, using the Risk-UE vulnerability index method. Bull Earthquake Eng, 8: 201–229

Leggieri V, Mastrodonato G, Uva G (2022). GIS Multisource data for the seismic vulnerability assessment of buildings at the urban scale. Buildings, 12(5): 523

Li S, Zhang Y, Du Z, Zhai C, Xie L (2014). Quantitative evaluation on building collapse induced human casualty for performance-based earthquake engineering. In: Liu X, Ang A H S, eds. Sustainable Development of Critical Infrastructure. New York: American Society of Civil Engineers

Li X, Li Z, Yang J, Liu Y, Fu B, Qi W, Fan X (2018). Spatiotemporal characteristics of earthquake disaster losses in China from 1993 to 2016. Nat Hazards, 94(2): 843–865

Liao Y H, Hwang L C, Chang C C, Hong Y J, Lee I N, Huang J H, Lin S F, Shen M, Lin C H, Gau Y Y, Yang C T (2003). Building collapse and human deaths resulting from the Chi-Chi Earthquake in Taiwan, September 1999. Arch Environ Health, 58(9): 572–578

Liu Y H, Li Z, Wei B, Li X, Fu B (2019). Seismic vulnerability assessment at urban scale using data mining and GIScience technology: application to Urumqi (China). Geomatics Nat Hazards Risk, 10(1): 958–985

Liu Y, So E, Li Z, Su G, Gross L, Li X, Qi W, Yang F, Fu B, Yalikun A, Wu L (2020). Scenario-based seismic vulnerability and hazard

analyses to help direct disaster risk reduction in rural Weinan, China. Int J Disaster Risk Reduct, 48: 101577

Liu Y, Zhang X, Liu W, Lin Y, Su F, Cui J, Wei B, Cheng H, Gross L (2023). Seismic vulnerability and risk assessment at the urban scale using support vector machine and GIScience technology: a case study of the Lixia District in Jinan City, China. Geomatics Nat Hazards Risk, 14(1): 2173663

Milutinovic Z V, Trendafiloski G S (2003). Risk-UE An advanced approach to earthquake risk scenarios with applications to different european towns. Contract: EVK4-CT–00014, WP4: Vulnerability of Current Buildings

Miura H, Midorikawa S (2006). Updating GIS building inventory data using high-resolution satellite images for earthquake damage assessment: application to metro Manila, Philippines. Earthq Spectra, 22(1): 151–168

Mouroux P, Le Brun B (2006). Presentation of RISK-UE project. Bull Earthquake Eng, 4(4): 323–339

Mueller M, Segl K, Heiden U, Kaufmann H (2006). Potential of high-resolution satellite data in the context of vulnerability of buildings. Nat Hazards, 38(1−2): 247–258

Papazafeiropoulos G, Plevris V (2023). Kahramanmaras-Gaziantep, Turkiye Mw 7.8 earthquake on February 6, 2023: strong ground motion and building response estimations. Buildings, 13(5): 1194

Perez J S, Llamas D C E, Dizon M P, Buhay D J L, Legaspi C J M, Lagunsad K D B, Constantino R C C, De Leon R J B, Quimson M M Y, Rhommel N G, Pitapit R S D, Rocamora C G H, Pedrosa M G G (2023). Impacts and causative fault of the 2022 magnitude (Mw) 7.0 Northwestern Luzon earthquake, Philippines. Front Earth Science, 11: 1091595

Polese M, d'Aragona M G, Prota A (2019). Simplified approach for building inventory and seismic damage assessment at the territorial scale: an application for a town in southern Italy. Soil Dyn Earthquake Eng Struct Dyn, 121: 405–420

Pourghasemi H R, Jirandeh A G, Pradhan B, Xu C, Gokceoglu C (2013). Landslide susceptibility mapping using support vector machine and GIS at the Golestan Province, Iran. J Earth Syst Sci, 122(2): 349–369

Riedel I, Guéguen P, Dalla Mura M, Pathier E, Leduc T, Chanussot J (2015). Seismic vulnerability assessment of urban environments in moderate-to-low seismic hazard regions using association rule learning and support vector machine methods. Nat Hazards, 76(2): 1111–1141

Ródenas J L, García-Ayllón S, Tomás A (2018). Estimation of the buildings seismic vulnerability: a methodological proposal for planning ante-earthquake scenarios in urban areas. Appl Sci (Basel), 8(7): 1208

Romano F, Zucconi M, Imperatore S, Ferracuti B (2017). Advancements in seismic vulnerability assessment methodologies for RC buildings at territorial scale. In: Advancement in Seismic Vulnerability Assessment Methodologies for Buildings at Territorial Scale. Pisa: Pisa University Press, 303–313

Ruggieri S, Calò M, Cardellicchio A, Uva G (2022). Analytical-mechanical based framework for seismic overall fragility analysis of existing RC buildings in town compartments. Bull Earthquake Eng, 20(15): 8179–8216

Ruggieri S, Cardellicchio A, Leggieri V, Uva G (2021). Machine-learning based vulnerability analysis of existing buildings. Autom Construct, 132: 103936

Salazar L G F, Ferreira T M (2020). Seismic vulnerability assessment of historic constructions in the downtown of Mexico City. Sustainability, 12(3): 1276

Schwenker F, Kestler H A, Palm G (2001). Three learning phases for radial-basis-function networks. Neural Netw, 14(4−5): 439–458

Susmaga R (2004). Confusion matrix visualization. In: IIPWM '04 Conference Proceedings of the International IIS: Intelligent Information Processing and Web Mining, Poland. Springer

Tesfamariam S, Liu Z (2010). Earthquake induced damage classification for reinforced concrete buildings. Struct Saf, 32(2): 154–164

Tilio L Murgante B, Di Trani F, Vona M, Masi A (2011). Resilient city and seismic risk: a spatial multicriteria approach. In: Computational Science and Its Applications-ICCSA 2011. International Conference, Santander, Spain. Proceedings, Part I, 410–422

Tyagunov S, Stempniewski L, Grünthal G, Wahlström R, Zschau J (2004). Vulnerability and risk assessment for earthquake prone cities. In: 13th World Conference on Earthquake Engineering

Xu X, Wen X, Han Z, Chen G, Li ChuanY, Zheng W, Zhnag S, Ren Z, Xu C, Tan X (2013). Lushan M S7. 0 earthquake: a blind reserve-fault event. Chinese Sci Bull, 58(28): 3437–3443

Xu Y, Lu X, Tian Y, Huang Y (2022). Real-time seismic damage prediction and comparison of various ground motion intensity measures based on machine learning. J Earthquake Eng, 26(8): 4259–4279

Yang Y, Li J, Yang Y (2015). The research of the fast SVM classifier method. In: 2015 12th International Computer Conference on Wavelet Active Media Technology and Information Processing (ICCWAMTIP), IEEE

Yariyan P, Zabihi H, Wolf I D, Karami M, Amiriyan S (2020). Earthquake risk assessment using an integrated fuzzy analytic hierarchy process with artificial neural networks based on GIS: a case study of Sanandaj in Iran. Int J Disaster Risk Reduct, 50: 101705

Yepes-Estrada C, Silva V, Valcárcel J, Acevedo A B, Tarque N, Hube M A, Coronel G, María H S (2017). Modeling the residential building inventory in South America for seismic risk assessment. Earthq Spectra, 33(1): 299–322

Zhang Z, Liu F, Zhao X, Wang X, Shi L, Xu J, Yu S, Wen Q, Zuo L, Yi L, Hu S, Liu B (2018). Urban expansion in China based on remote sensing technology: a review. Chin Geogr Sci, 28(5): 727–743

Zuccaro G, Cacace F (2015). Seismic vulnerability assessment based on typological characteristics. The first level procedure "SAVE". Soil Dyn Earthquake Eng, 69: 262–269